Physical Aspects of Microwave and Radar Applications

Antenna Beam Broadening in Multifunction Phased Array Radar

R. Fatemi Mofrad* and R.A. Sadeghzadeh

Electrical & Computer Engineering Department, K.N. Toosi University of Technology, Tehran, Iran

A phased array antenna is designed for multifunction phased array radar simulation test bed. Effect of element pattern, mutual coupling between elements, phase quantization, amplitude and phase error and elements failure rates on array pattern are discussed. Target angle measurement and side lobe cancelling, in order to reduce jamming power through side lobes, is illustrated in this antenna. Also antenna beam width is broadened with different methods and compared with narrow beam characteristics. It is shown that, for special broadening factors, beam broadening may lead to a better coverage and power efficiency relative to narrow beam antenna.

PACS: 84.40.Ba, 84.40.Xb, 84.40.Ua

1. Introduction

Phased array antennas have matured rapidly in recent years and this technology is set to become the norm in complex and advanced radar systems. The ability to steer the radar beam electronically allows a combination of functions, such as tracking, surveillance and weapon guidance, which were traditionally performed by dedicated individual radars. This new type of radar is called multifunction array radar (MFAR). In these radars, effect of different antenna beam characteristics (e.g. beam width) or tracking algorithms on the overall radar performance need to be done based on realistic simulations, because these sophisticated radars cannot be tested completely in real world. These realistic simulations should have two main properties: first to include different aspects of real operational scenarios facing MFAR as much and accurate as possible. The second is that these simulations should provide the facility to model different part of a MFAR in order to evaluate the performance of each section in the radar as a whole system (to consider the interaction between subsystems). MFAR simulation test bed is a software tool for MFAR designers to design and evaluate the performance of such kind of sophisticated radars [1]. In the MFAR simulation test bed, active phased array radar, with specification in Table I, is considered as a pilot for different radar resource management, target tracking and beam forming algorithms comparison and development. In this simulation test bed, transmitting and receiving chain, antenna structure and signal processing algorithms are fixed. User may write his or her own radar resource management, target tracking and beam forming algorithms and after defining appropriate operational scenarios, assess results of the designed algorithms. The most important part of this simulation test bed is a phased array antenna. That is an active phased array with about 5000 elements. It is assumed that digital beam forming is possible at element level and so designer may design appropriate beam forming algorithms and evaluate the results on radar performances.

TABLE I

MFAR characteristics.

MFAR parameter	Value
angle tracking accuracy	12′
antenna scanning range in az. and el.	−45°– +45°
antenna tilt angle	0–45°
frequency band	S
antenna beamwidth	1.5° × 1.7°
polarization	vertical
antenna gain	40 dB
sum pattern side lobe level	30 dB
difference pattern side lobe level	20 dB
number of T/R modules	5000

In this paper, a narrow pencil beam with capability to measure azimuth and elevation angles of target and side lobe cancelling in the presence of jamming is designed for this simulation test bed. Effect of element pattern, phase quantization, amplitude and phase error, elements failure rates on array pattern and mutual coupling between elements, are presented. The narrow beam width is usually designed to meet tracking requirements of a MFAR (resolution and accuracy). Search of a large area by this narrow beam becomes too time consuming. In these occasions antenna beam broadening is useful.

In this paper antenna beam width is broadened and compared with narrow beam characteristics. It is shown that, for special broadening factors, beam broadening may lead to a better coverage and power efficiency relative to narrow beam antenna.

* corresponding author; e-mail: rfatemim@yahoo.com

2. Planar array structure

For scanning in elevation and azimuth planar array should be used. Details of planar array theory are given in available texts [2–4]. All the antenna elements have a certain element pattern $e(\theta, \varphi)$. This is multiplied with the array factor resulting in the final antenna pattern $E(\theta, \varphi)$ (field strength):

$$E(\theta,\varphi) = e(\theta,\varphi) f(\theta,\varphi) . \quad (1)$$

Array antennas often use rectangular or triangular placement of elements. Usually an array with a triangular grating, particularly an equiangular one, is preferred. This arrangement reduces the number of elements by nearly 13% and increases the area associated to each element [5]. Designed array has a rectangular aperture with 80 elements in azimuth and 64 elements in elevation direction, so an asymmetrical pattern in H and E planes is produced.

The maximum distance between radiators of a scanning antenna array is related to the maximum angle of deviation of the pattern. For $\pm 45°$ electronic steering, distance between elements is designed to be equal to 0.58λ which will not generate grating lobes. With this selection, dimension of aperture will be: 4.64 m $\times$ 3.71 m. There are many weighting window types with different properties. In the Taylor tapering there is a better tradeoff between decrease in the side lobe level and broadening the main beam [3]. Amplitude weighting, at T/R module level leads to more complication of the modules (controllable attenuators and phase shifters will be needed).

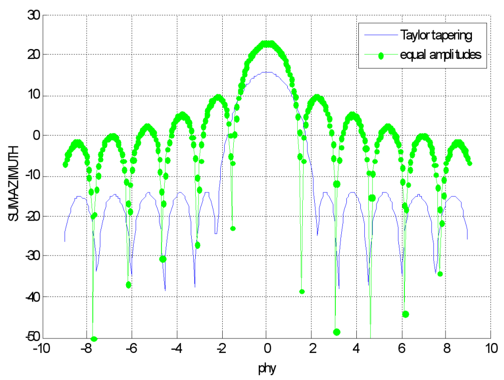

Fig. 1. Array pattern with and without Taylor tapering.

For difference pattern generation, the aperture can be derived with the Bayliss tapering [3]. The Bayliss tapering is applied at output of 160 sub-arrays each with 4×8 elements [6]. The Bayliss amplitude tapering at sub-array level will increase side lobe level of difference pattern relative to sum pattern. Usually target detection and acquisition is performed by sum pattern, so higher side lobe level in the difference pattern would not cause false alarm due to clutter or other unwanted targets.

The radiated pattern of antenna array with and without amplitude tapering is shown in Fig. 1. With tapering, side lobe level will decrease by about 16 dB. In the transmission mode the aperture of antenna array should operate with uniform amplitude illumination. In this way maximum possible power of transmitter modules will be derived with maximum efficiency.

3. Angle measurement

In this antenna, monopulse likelihood function is used for direction estimation of target [2]. In likelihood estimation there is a tapering to form difference pattern. This tapering equals to the coordinates of element which are distributed symmetrically around axis. This tapering in comparison to the Bayliss tapering produces sharper difference pattern and increases accuracy of angle estimation but with higher side lobes. By multiplying Bayliss tapering with this tapering, sharpness of difference pattern will decrease but lower side lobes will be produced. The characteristics of this mixed tapering are a tradeoff between selection of the Bayliss and likelihood estimation tapering. An example of direction estimation is shown in Fig. 2 for beam direction at 35° in azimuth and elevation. Figure 3 depicts standard deviation of target direction es-

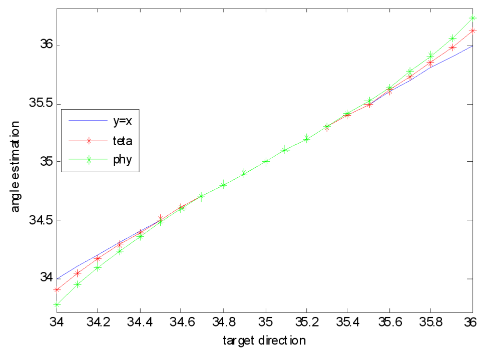

Fig. 2. Direction estimation for beam direction at 35° (SNR = 10).

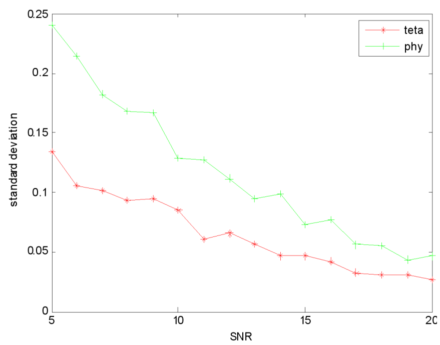

Fig. 3. Standard deviation of target direction estimation (in degree) as a function of signal to noise ratio (SNR) (in dB).

timation as a function of SNR. These results well match with similar results in [2].

4. Digital phase shifter

Usually digital phase shifters, characterized by the number of bits M, are used for beam steering. M determines the residual phase error within the interval: $\Delta\varphi = \pm\pi/2^M$. The main effect of discrete phase shifting is on side lobes. In Fig. 4 simulation results show increase in side lobe level (SLL) with 4 type of discrete phase shifters. These results well match with those in [2]. According to these results, 6 bits phase shifter has satisfactory results.

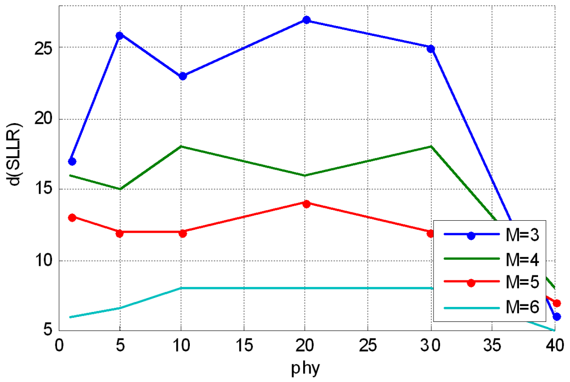

Fig. 4. Increase of side lobe level ratio (SLLR) (in dB) versus scan angle (in degree) with discrete phase shifter.

5. Element pattern effect

Parameter of the designed microstrip patch antenna at 3 GHz are [6, 7]:

$$\varepsilon_r = 2.1\,,\quad L = W = 0.39\lambda_0\,,\quad d = 0.06\lambda_0\,. \tag{2}$$

In Eq. (2), d is height of substrate, ε_r is dielectric constant of substrate and L and W are dimensions of patch. Half power beam width of element is 80 degree, so there is 3 dB loss of effective radiated power (sum of gain and radiated power) at ±40 degrees steering angles. The effect of element pattern loss together with beam broadening loss due to beam steering is depicted in Fig. 5. This result well matches with those in [8].

6. 20% failure rate of elements

When 20% of elements accidentally turn off, side lobe level will increase. Figure 6 compares array pattern in this condition with main array pattern. Simulation results show that in the worse condition there is 22 dB increase in side lobe level of sum pattern and 14 dB in difference. The effect of failure on the gain and beam direction is negligible.

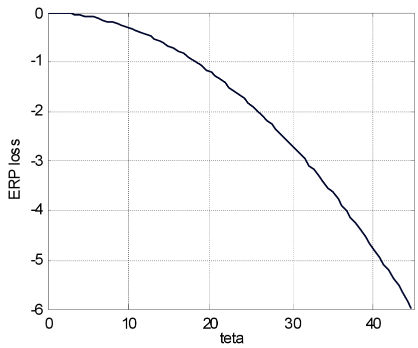

Fig. 5. Decrease of effective radiated power (ERP) (in dB) with scan angle (in degree) because of both element pattern and beam broadening in E-plane.

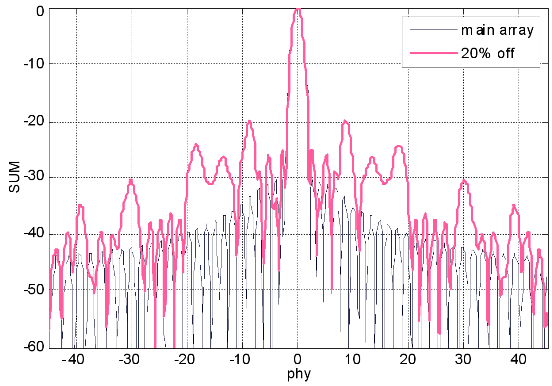

Fig. 6. Array pattern (in dB) versus scan angle (in degree) for 20% failure of elements (160 subarray).

7. Amplitude and phase error

Simulation results show that with 40% amplitude tolerance there is 2 dB increase in side lobe level. This error is independent of steering angle. Also it has been shown that destructive effect of phase error is more than amplitude error. Its main effects are loss in the effective radiated power and increase in side lobe level. According to simulation results, maximum tolerable phase error is about $0.5 \approx 0.25$ rad.

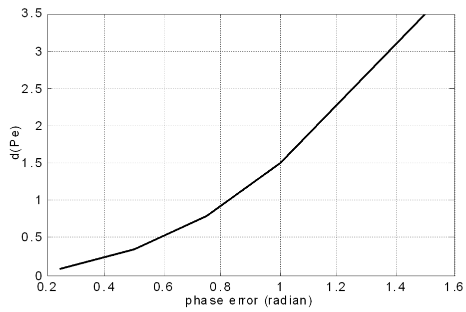

Fig. 7. Decrease of ERP (in dB) with increase of phase tolerance.

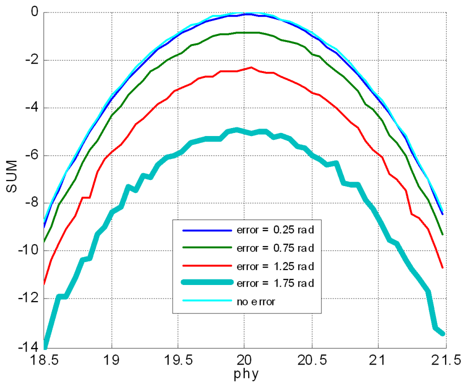

Fig. 8. Increase in main beam ripples (in dB) versus scan angle (in degree) with increase of phase tolerance.

Figure 7 shows loss of maximum effective power with increase in phase error. Phase error causes ripples in main beam and with increasing in phase error these ripples may be seen clearly.

This effect is shown in Fig. 8. In this figure decrease of effective radiated power is also shown. This power distributes in side lobes. Side lobes that are far from bore side are higher in comparison with pattern that has no phase error.

8. Side lobe canceller

The Widrow–Hoff least mean square (LMS), side lobe canceller (SLC) algorithm, which is a closed loop digital algorithm described by [2, 9] was implemented in the simulation test bed. The benefit of using the SLC can be measured by jammer cancellation ratio (CR), defined as the ratio of the output noise power with and without the SLC. For instance the CR value obtained in this simulation test bed with one channel SLC is about 30 dB for a jammer at 14.5° azimuth angle.

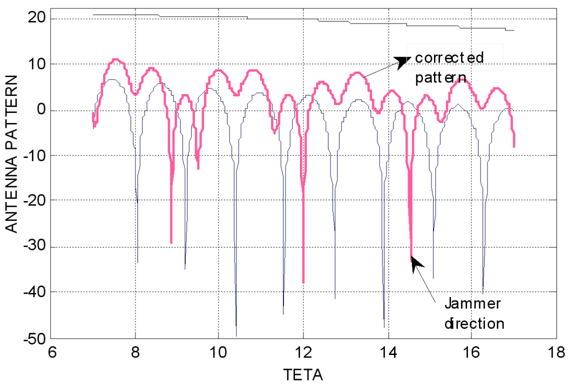

Fig. 9. Adopted pattern (dotted line) and main pattern (continuous line) with one auxiliary antenna for jammer incoming at 14.5° azimuth.

Figure 9 shows adapted antenna pattern obtained by this LMS algorithm. The gain margin of auxiliary SLC antenna with respect to the side lobe gain of the radar antenna in the jammer direction is an important parameter. A large value of the gain margin in the steady-state of an adaptive SLC would be desirable. However, in the transient state of the SLC a low value of gain margin would be advisable. A compromise value is around 10 dB for the gain margin. In Fig. 9 half power beam width of auxiliary antenna cover ±15° around bore sight and so its gain will be 16 dB that is 6 dB more than side lobe level.

9. Mutual coupling effect

Microstrip patch is a main candidate to be used as the elements of integrated phased arrays. Such arrays may include active devices on the same or on a parallel substrate, integrated monolithically or in a hybrid fashion. Design of these arrays depends on understanding of the effects of substrate thickness, dielectric constant, and grid spacing on the scan performance of the beam. The scan performance means the active reflection coefficient magnitude, with the array matched at broadside and is directly related to the active element pattern. For an array of printed patch antenna, scan blindness is possible whenever the wave number coincides with the propagation constant of a surface wave on the structure. Scan blindness will occur if the following three conditions are satisfied [10]:

1) The propagation constant equals surface wave propagation constant.

2) The grid spacings $\mathrm{d}x$, $\mathrm{d}y$ are such that the equality of propagation constant in (1) occurs for values of u, v in real space.

3) The pole of TM (TE) surface wave in (1) is not cancelled by a zero value of kx (ky).

Mathematically, condition (1) can be expressed as

$$\left(\frac{\beta_{\mathrm{SW}}}{k_0}\right)^2 = \left(\frac{k_x}{k_0}\right)^2 + \left(\frac{k_y}{k_0}\right)^2 = \left(\frac{m}{\mathrm{d}x/\lambda_0} + \sin\theta_0\cos\varphi_0\right)^2 + \left(\frac{n}{\mathrm{d}y/\lambda_0} + \sin\theta_0\sin\varphi_0\right)^2. \tag{3}$$

In Eq. (3) λ_0 is the free space wavelength. Physically, the cancellation condition referred to in (3) means that the polarization of the array is such that the particular TM or TE surface wave cannot be excited.

Figure 10 shows blind point versus space between elements of designed arrays (with patch length and width $L = W = 0.39\lambda_0$, substrate thickness $d = 0.06\lambda_0$, and substrate permittivity $\varepsilon_r = 2.1$). The blind spot position moves toward broadside by increase in the space between elements. With $\mathrm{d}x = \mathrm{d}y = 0.58\lambda$, the array has a scan blindness in the E-plane at 44.76°. With $\mathrm{d}x = \mathrm{d}y = 0.51\lambda$ blind spot moves to 70° that is a better

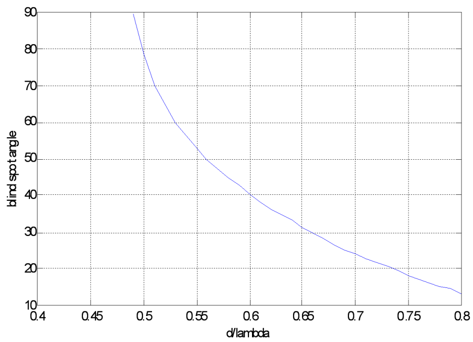

Fig. 10. Blind angle (in degree) versus space between elements.

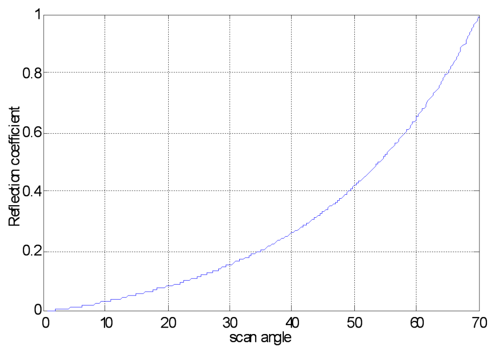

Fig. 11. Reflection coefficient versus scan angle $dx = 0.51\lambda$, $dy = 0.51$.

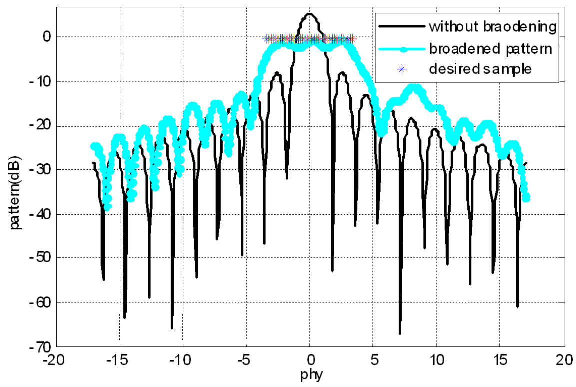

Fig. 12. Narrow and broadened beam patterns.

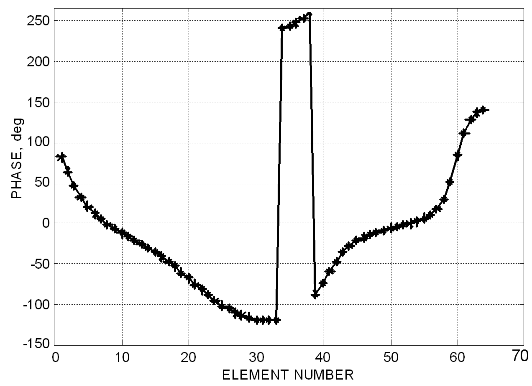

Fig. 13. Phase of elements in broadened beam antenna.

choice for an array with $\pm 45°$ scanning angle. In this case the magnitude of the reflection coefficient at $45°$ is about 0.3 and then the loss of power gain will be only 0.4 dB.

Figure 11 shows the magnitude of the reflection coefficient of a patch in designed array with spacings $dx = dy = 0.5\lambda$. These results well match with those in [3].

10. Beam broadening

As was said before, in the transmission mode the aperture of antenna array should operate with uniform amplitude illumination. In this way maximum possible power of transmitter modules will be derived with maximum efficiency. So transmit beam broadening should be done with uniform amplitude and phase only tapering. Broadening factor is defined as broadened 3 dB beam width to narrow 3 dB beam width. In the MFAR simulation test bed, a broadening factor of 4 in elevation angle is desired so broadening should be done by linear array with 64 elements. Gradient search algorithm (GSA) [11] is used for broadening of the linear array.

In Fig. 12 pattern of broadened and narrow beams are presented and compared.

Figure 13 shows required phase of elements for beam broadening. This phase is calculated by GSA. A good measure of comparison between two patterns, is beam power efficiency which is defined as the ratio of transmitted power in the 3 dB main lobe of broadened beam to narrow beam. With beam broadening, it is possible to radiate more power into space so a beam power efficiency more than one is achieved. Beam efficiency for three linear arrays:

— a linear array with 64 elements and $\lambda = 0.1$,

— a linear array with 64 elements and $\lambda = 1$,

— a linear array with 80 elements and $\lambda = 1$

is presented in Fig. 14 for broadening factors up to 15. As is clear, for broadening factors more than 2.5, beam power efficiency becomes more than 1 (0 dB).

With beam broadening, space coverage is also increased. In Fig. 15 from [12] space coverage of a narrow beam of width equal to 1 is $\pi/4$. This coverage for a 1×4 broadened beam is $3 + \pi/4$. There is a coverage difference of $3 - 3\pi/4$ between coverage of two beams. In the other word, broadened beam approximately cover 20% $(0.6438/\pi)$ of environment. This improvement in coverage is for none overlapped beams. For overlapped beams this improvement will increase appropriately.

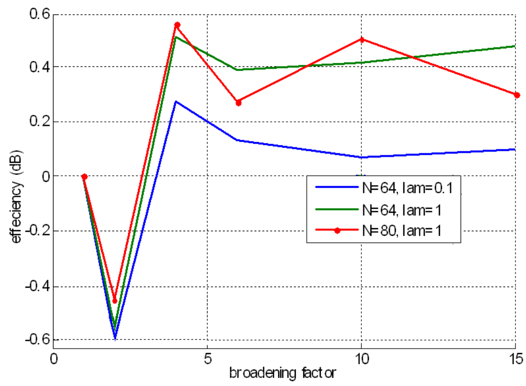

Fig. 14. Beam power efficiency vs. broadening factor.

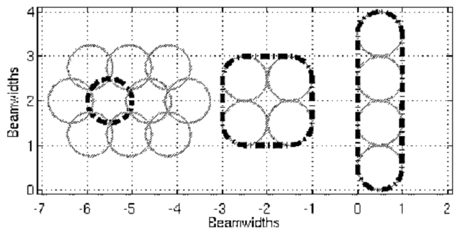

Fig. 15. Coverage area of different patterns.

Beam broadening is also possible with amplitude and amplitude–phase tapering methods. These two methods yield better side lobe levels and lower error between required and achieved patterns. However as was said before, amplitude tapering would lead to power losses. Among these two methods, amplitude–phase tapering yields better side lobe levels and lower dynamic range between elements amplitudes. Lower dynamic range between element amplitudes leads to lower mutual coupling. A comparison of three tapering methods in antenna beam broadening is shown in Table II. Pattern error in Table II is difference between required and achieved patterns.

11. Conclusion

In this paper, design of antenna section of multifunction phased array radar simulation test bed was illustrated. Effect of element pattern, phase quantization, amplitude and phase error and elements failure rate on array pattern was presented. Antenna beam broadening was illustrated and compared with three different tapering methods. It was shown that phase only tapering is appropriate for MFAR transmit beam broadening. Beam broadening increases the space coverage and power transmission in the antenna main lobe. These will lead to better search performance of MFAR. Effect of different antenna parameters can easily be evaluated by a little change in multifunction phased array radar simulation test bed program. In this way, design of the antenna (e.g. required side lobe level in the electronic warfare scenarios or SLC performance and angle measurement accuracy) may be finalized in real scenario simulations. Future works includes search function performance comparison between MFARs with narrow and wide antenna patterns.

TABLE II

Comparison between three beam broadening methods.

	Amplitude tapering	Phase tapering	Amplitude–phase tapering
relative directivity [dB]	−6	−6	−6
efficiency [dB]	−8.8	0.3	−0.3
rms of beam error	0.0889	0.0977	0.095
beam ripple [dB]	0.4	1.7	1.4
side lobe level [dB]	16	13	14.4

References

[1] R. Fatemi Mofrad, R.A. Sadeghzadeh, in: *Proc. Int. Radar Symp., Vilnius (Lithuania)*, 2010, p. 265.

[2] W.D. Wirth, *Radar Techniques Using Array Antennas*, The Institution of Electrical Engineers, 2001.

[3] R.C. Hansen, *Phased Array Antennas*, Wiley, New York 2001.

[4] R.J. Mailloux, *Phased Array Antenna Handbook*, Artech House, 2005.

[5] E.D. Sharp, *IEEE Trans. Antenna Propag.* **AP-9**, 126 (1961).

[6] I.J. Bahe, P. Bhartia, *Micro Strip Antenna*, Artech House, 1980.

[7] R. Garg, P. Bhartia, I. Bahl, A. Ittipiboon, *Design Handbook of Micro Strip Antenna*, Artech House, 2001.

[8] B.K. Sarkar, *Effect of element characteristics on the scanning range of phased array radar* in: *Proc. IEEE Radar Conf.*, IEEE, 2006.

[9] A. Farina, *Antenna-Based Signal Processing Techniques for Radar Systems*, Artech House, 1994.

[10] D.M. Pozar, *IEEE Trans. Antenna Propag.* **AP-32**, (June 1984).

[11] A.K. Bhattacharyya, *Phased Array Antenna Floquet Analysis, Synthesis, BFNs, and Active Array System*, Wiley, 2006.

[12] J.C. Kerce, G.C. Brown, M.A. Mitchell, in: *Fourth IEEE Workshop on Sensor Array and Multi-Channel Processing (SAM-2006), Waltham (MA)*, IEEE, 2006.